Discovery of the Linear Carbon Chain Molecules ^{13}CCC and C^{13}CC Towards SgrB2(M)

Thomas Giesen

Laboratory for Astrophysics, Institute of Physics, University of Kassel, Kassel D-34132, Germany

SOFIA GREAT Receiver

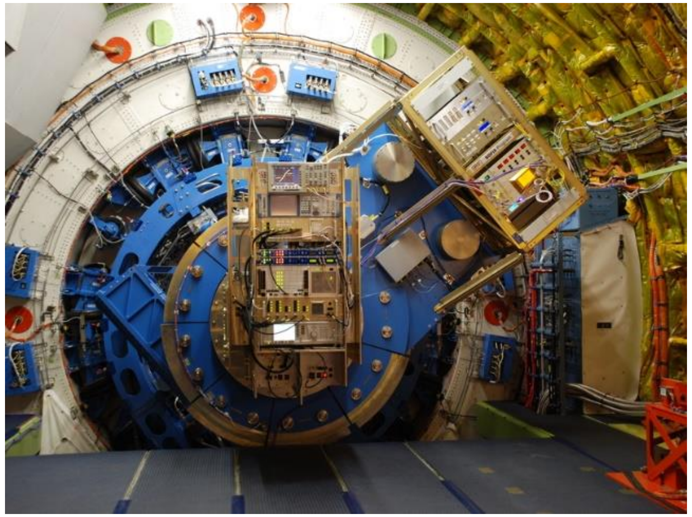

Front-End: LFAH	Frequencies (GHz)	Lines of Interest
Two 7-pixel arrays at two polarizations (H,V). Both polarizations can be tuned to the same frequency (LFAH range), or two separate frequencies on a best effort basis.	1835–2007	[CII] 158 µm, CO, OH, $^2\Pi_{1/2}$, ^{12}CH, ^{13}CH **NEW**: **C_3 ^{13}CCC C^{13}CC**

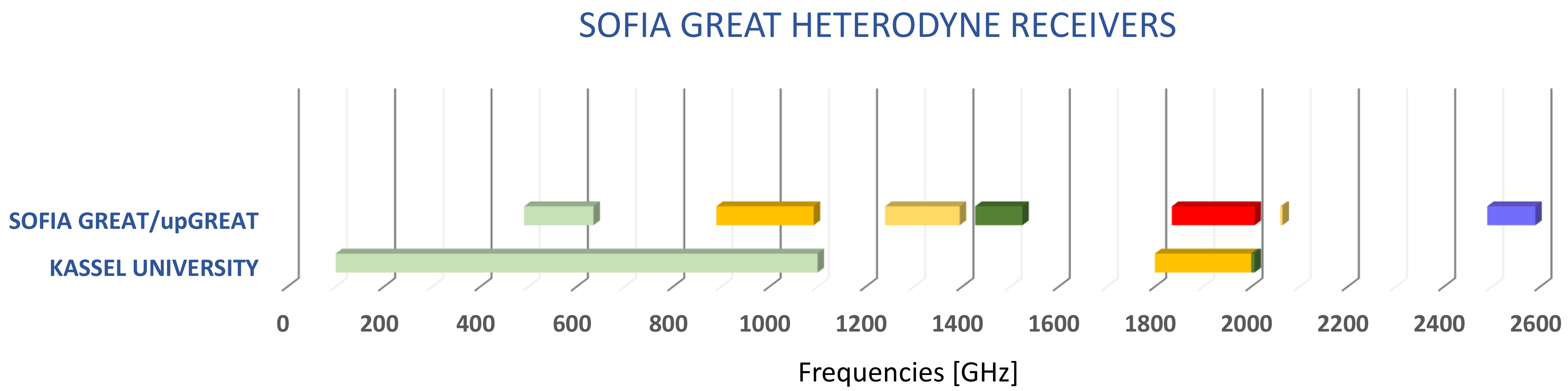

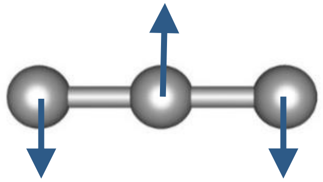

μ_{vib} = 0.4 Debye

Lowest bending vibration of C_3 at 1.9 THz

COSSTA Terahertz-Sideband Spectrometer / Cologne

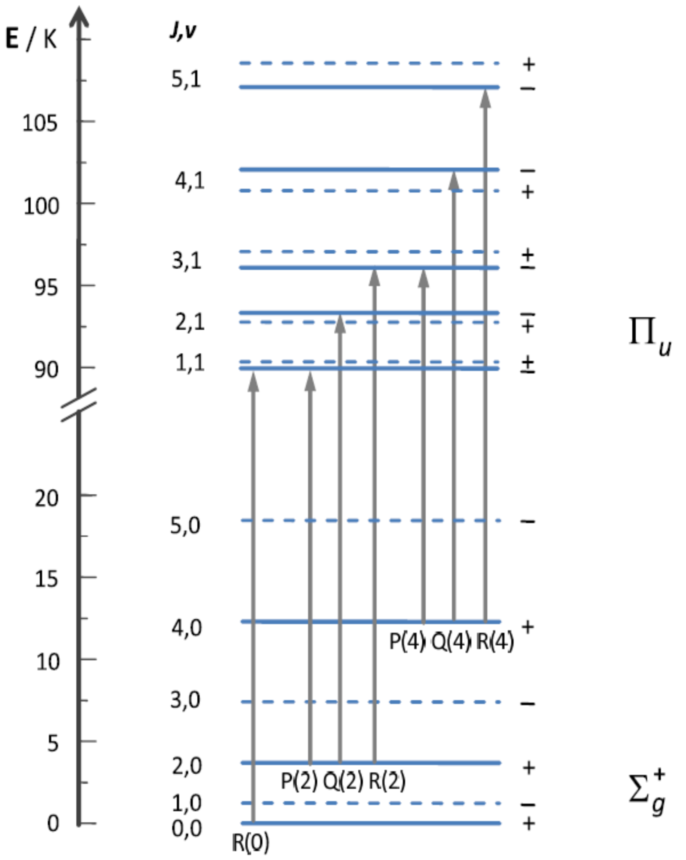

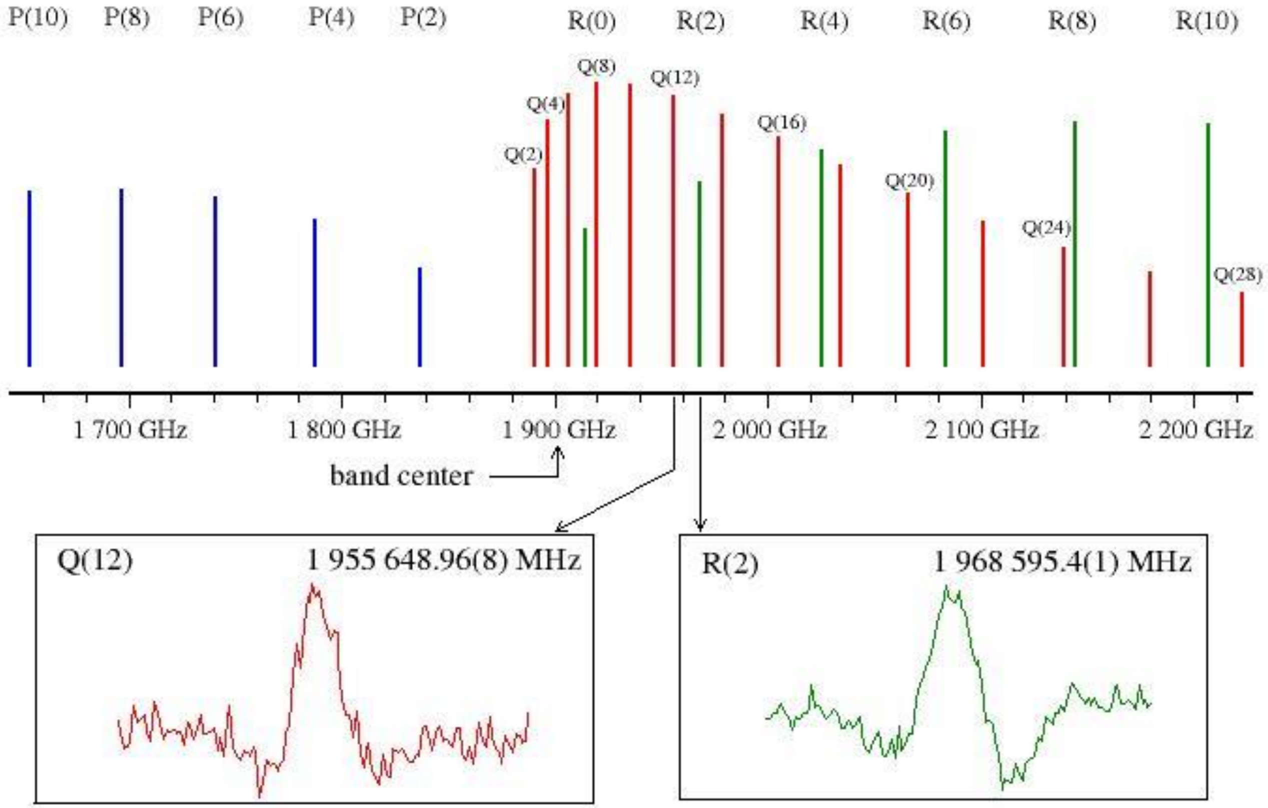

Selection Rules: ΔJ = - 1 0 +1

P(J) Q(J) R(J)

T.F. Giesen, A. O. Van Orden, J.D. Cruzan, R.A. Provencal, R.J. Saykally, R. Gendriesch, F. Lewen, G. Winnewisser, *Astrophys. J.* 551, L181, (2001)

Experimental setup at University of Kassel / Germany

Supersonic **Je**t **S**pectrometer for **T**erahertz **A**pplications (SuJeSTA)

Reaction Chamber

Lowest bending mode of ^{13}C-substituted C_3 and an experimentally derived structure

A.A. Breier, T. Büchling, R. Schnierer, V. Lutter, G.W. Fuchs, K.M.T. Yamada, B. Mookerjea, J. Stutzki, T.F. Giesen, J. Chem. Phys. 145, 23 (2016)

Laboratory Spectra of C_3 and its Isotopologues at 1.8 – 1.9 THz

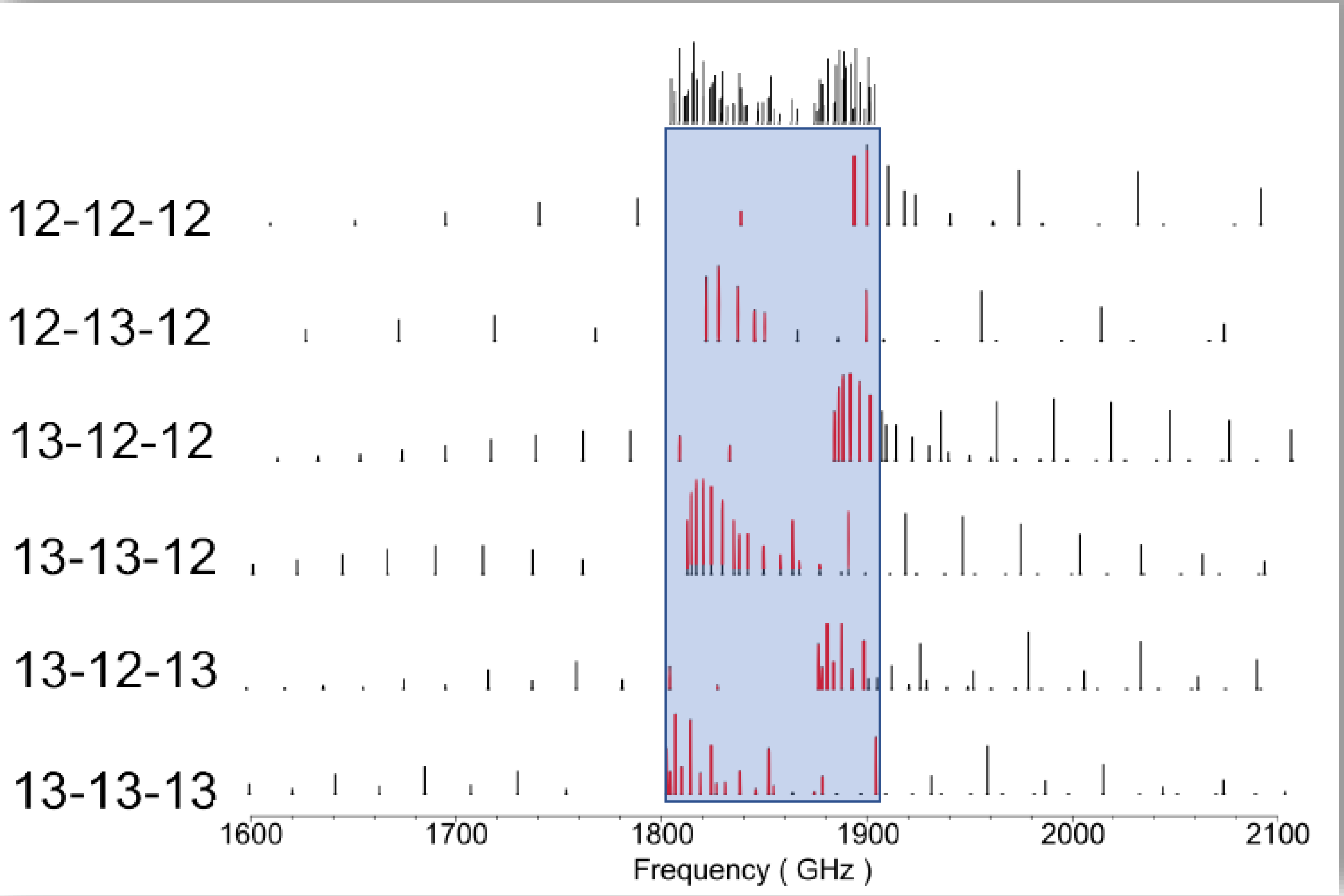

Laser Ablation of Graphite

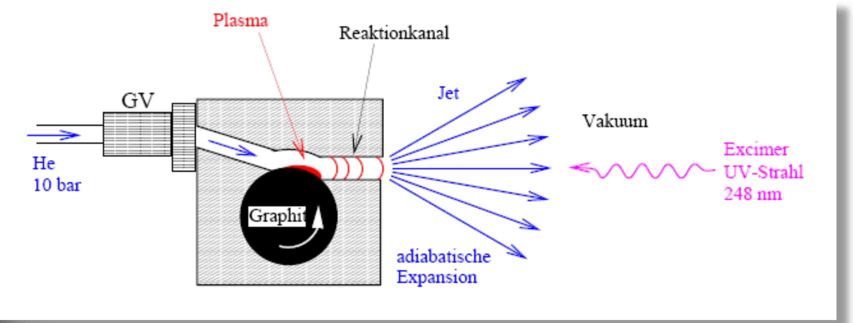

Supersonic Jet

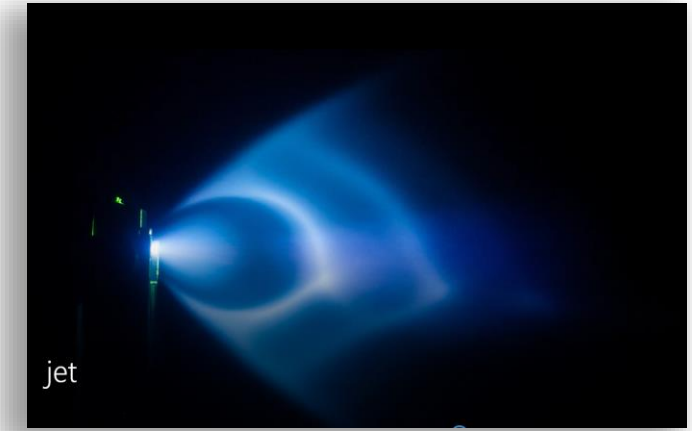

Photo by Björn Waßmuth

Abundances and Intensities of $^{12}C^{13}C^{12}C$ and $^{13}C^{12}C^{12}C$

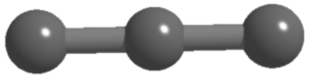

^{13}C Substitution

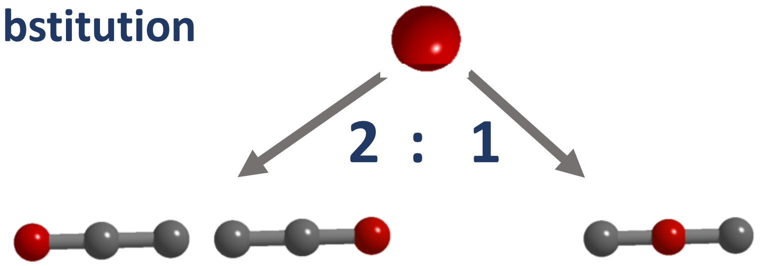

Partitionfunction $Q^{13CCC} : Q^{C13CC}$

2 : 1

Intensity of individual lines

$$I \sim \frac{N}{Q}$$

Line Inensity Ratio $I^{13CCC} : I^{C13CC}$

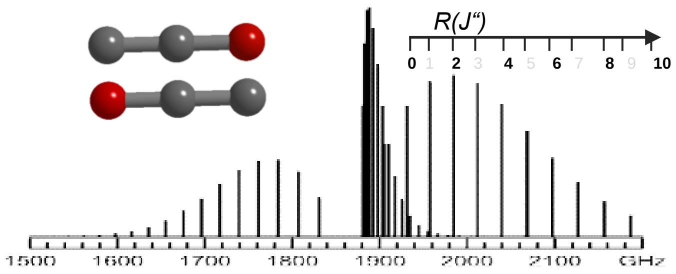

1 : 1

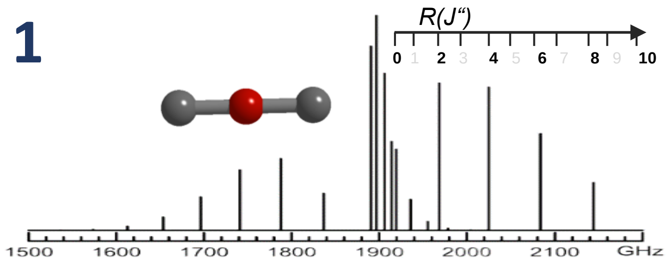

^{13}CCC and C^{13}CC observations

with SOFIA GREAT and upGREAT

Observations started from New Zealand

Target : SgrB2(M)

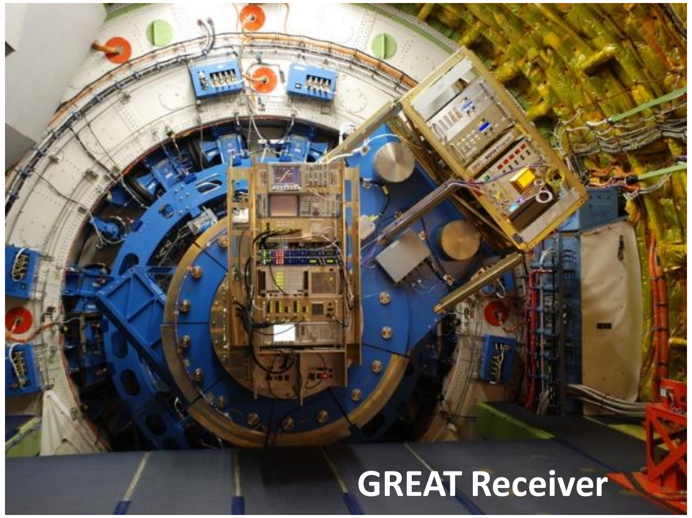

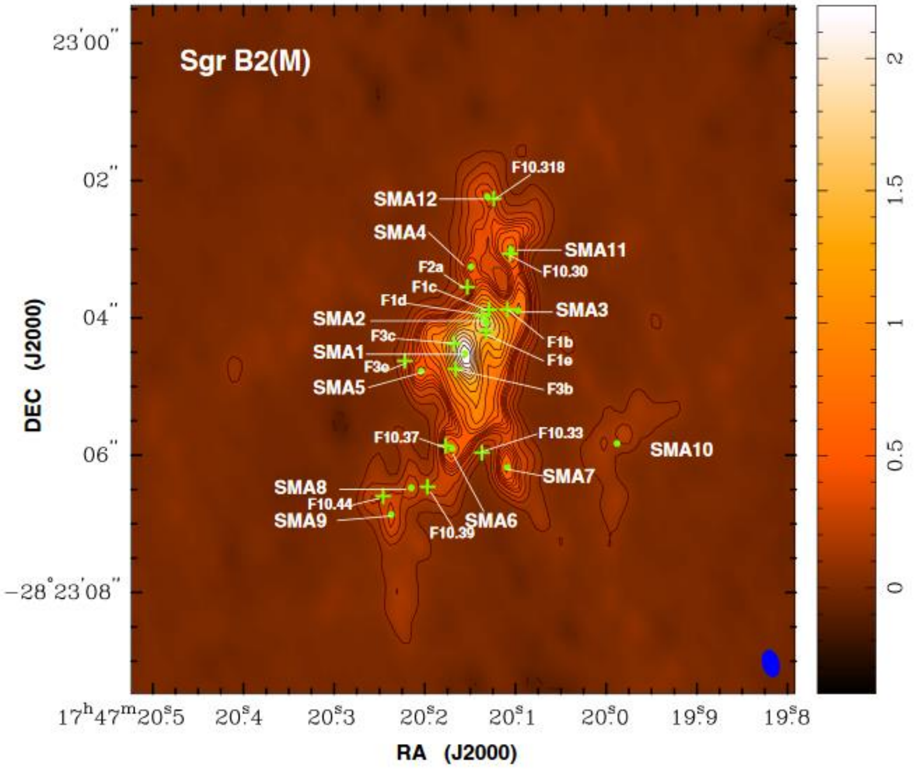

Data Analysis

-2015: CCC_Q(6), 13CCC_Q(2), 13CCC_Q(4) (3 tunings) during 40 minutes in-flight time

- 2016: 13CCC_Q(4) (one additional tuning) during 30 minutes in flight-time

averaged ^{13}CCC_Q(4) spectrum:
- 3 tunings from 2015
- 1 tuning from 2016, corrected for sideband absorption as derived from 2015 tunings

^{13}CCC_Q(2)
CCC_Q(6)

→ convincing detection of ^{13}CCC !
- two lines with consistent profile
- profile consistent with lower velocity component of C_3 absorption

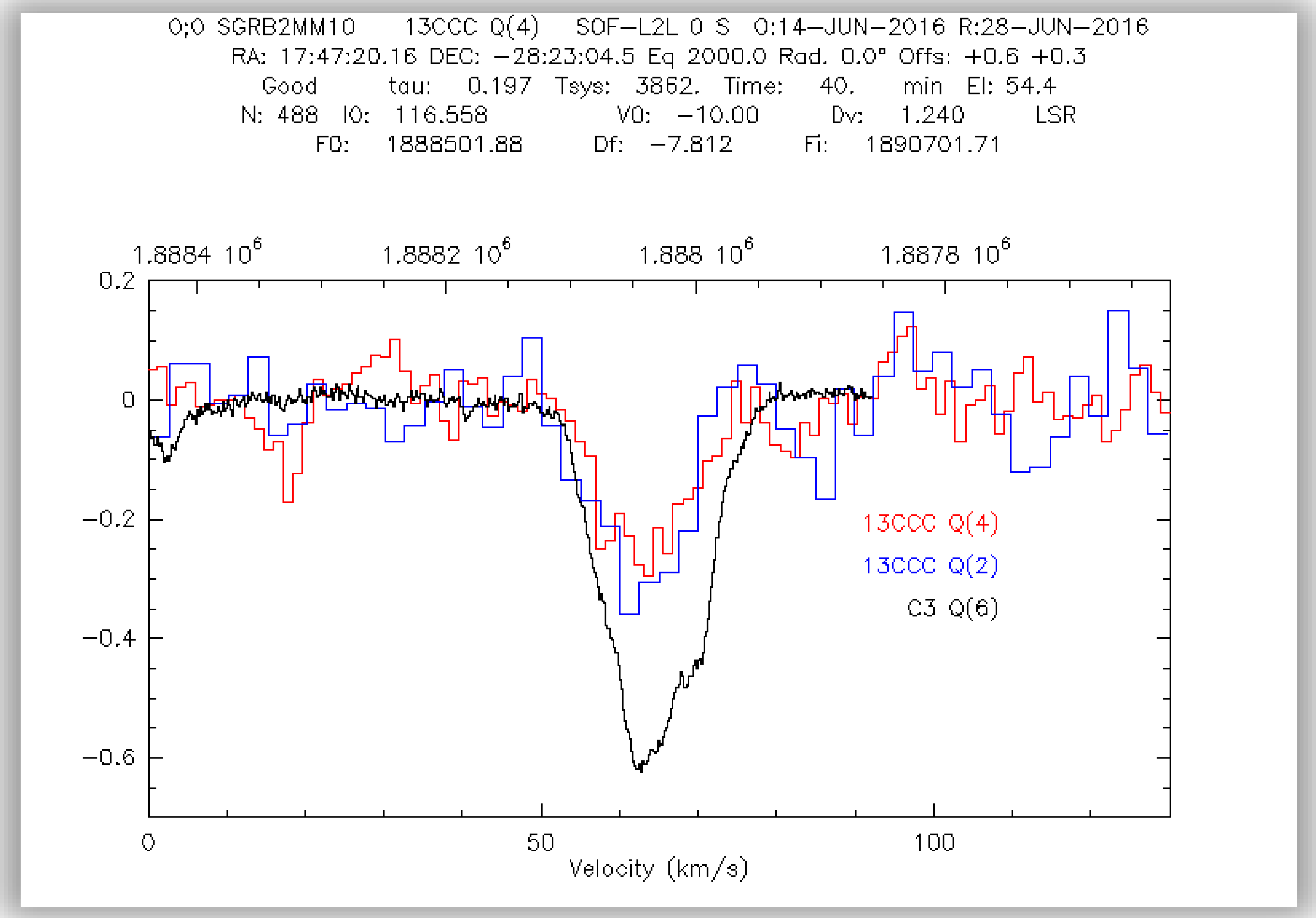

First Interstellar Detection of the Carbon Chain Molecules ^{13}CCC and $C^{13}CC$ toward SgrB2(M)

Parameters for Observed $C^{13}CC$ and ^{13}CCC

Transition	Frequency MHz	Einstein A_{ul} s^{-1}	E_l K	g_l	g_u
$C^{13}CC$					
Q(2)	1819596.013	0.01309	3.7	5	5
Q(4)	1825647.312	0.01322	12.4	9	9
^{13}CCC					
Q(2)	1882638.269	0.01450	3.7	5	5
Q(4)	1888501.880	0.01463	12.4	9	9

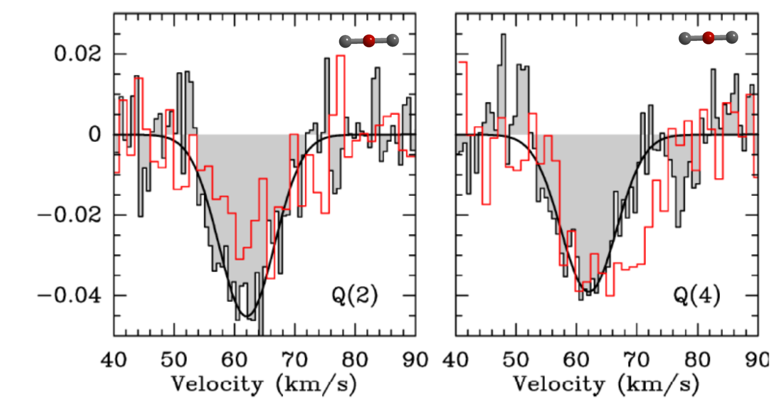

Ro-vibrational spectra of $C^{13}CC$ observed towards SgrB2(M)
H-polarization (filled spectrum), V-polarization (red).

$C^{13}CC$ and ^{13}CCC Observational Settings

SOFIA/GREAT (G) and upGREAT (upG) Receivers

Transition	Rec.	Obs. Date	υ^*_{off} km/s	T_{int} min	T_{rms} mK
^{13}CCC - Q(2)	G	19 July 2015	+10.0	6.8	99
^{13}CCC - Q(4)	G	19 July 2015	+0.0	27.9	62
	upG	9 June 2016	-10.0	12.5	96
$C^{13}CC$ - Q(2)	upG	28 June 2017	0.0	5.7	112
	upG	28 June 2017	+10.0	5.1	150
$C^{13}CC$ - Q(4)	upG	28 June 2017	0.0	8.5	56
	upG	28 June 2017	+10.0	2.8	150

* Velocity offset of LO setting relative to the υ_{LSR}

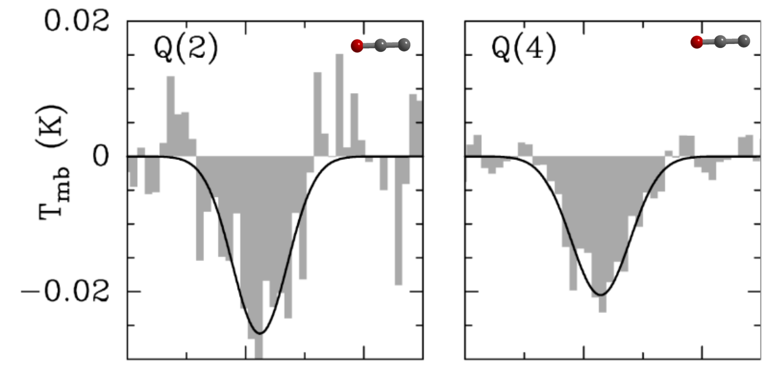

Ro-vibrational spectra of ^{13}CCC observed towards SgrB2(M)

T. F. Giesen, B. Mookerjea, G. W. Fuchs, A. A. Breier, D. Witsch, R. Simon, J. Stutzki, A&A 2020, **633,** A120

Ro-vibrational Transitions of the Main Isotopologue CCC

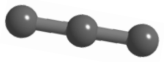

T. F. Giesen, B. Mookerjea, G. W. Fuchs, A. A. Breier, D. Witsch, R. Simon, J. Stutzki, A&A 2020, **633,** A120

Parameters for the Observed CCC Transitions.

Transition	Frequency MHz	Einstein A_{ul} s^{-1}	E_l K	g_l	g_u
CCC					
Q(2)	1890558.188	0.01468	3.7	5	5
Q(4)	1896706.838	0.01482	12.4	9	9
Q(6)	1906337.907	0.01505	26.0	13	13
P(2)	1836823.502	0.00449	3.7	5	3
P(4)	1787890.534	0.00532	12.4	9	7
P(6)	1741122.646	0.00521	26.0	13	11
P(8)	1696525.363	0.00495	44.6	17	15
P(10)	1654087.900	0.00466	68.1	21	19
P(12)	1613805.250	0.00437	96.6	25	23

Observed CCC Transitions in SgrB2(M)

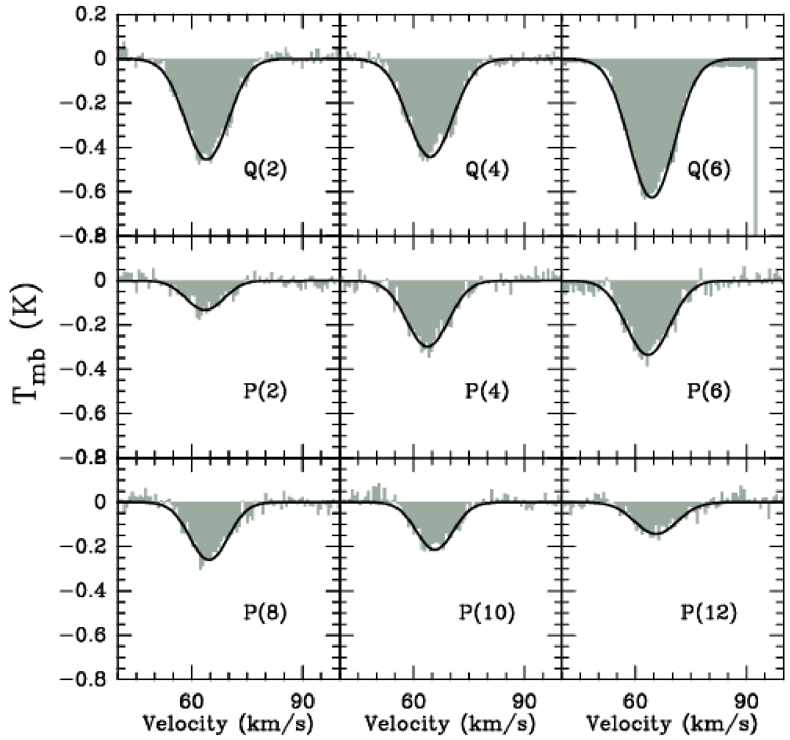

Temperature of CCC in SgrB2(M)

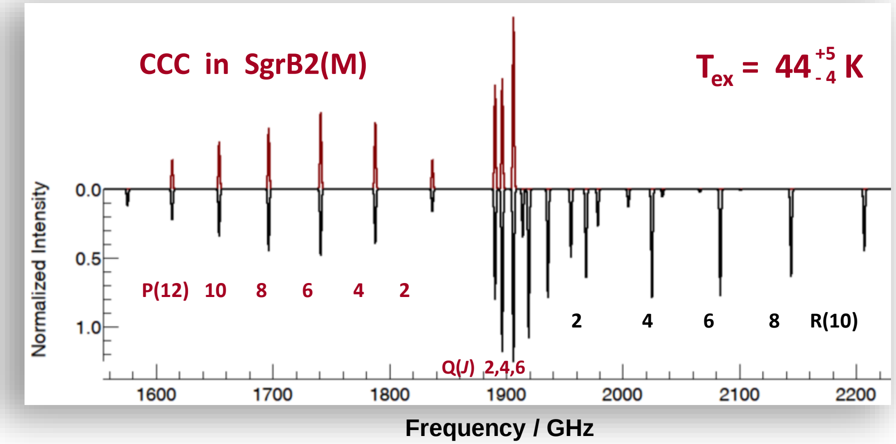

$$A_{\rm ul} = \frac{16\pi^3}{3\epsilon_0 h}\frac{\nu^3}{c^3}\cdot|\mu_{\rm lu}|^2 \quad \text{and} \quad |\mu_{\rm lu}|^2 = \frac{|\mu_{\rm v}|^2 L_{P/Q/R}(J)}{g_{\rm u}}$$

Hönl-London factors for Lin. Mol. of Π–Σ transitions:

$L_P(J) = J-1$, $L_Q(J) = 2J+1$, $L_R(J) = J+2$

Data Analysis of C_3 CCC, ^{13}CCC and C^{13}CC

Table 3. Summary of observed and derived quantities for the CCC, C^{13}CC, and ^{13}CCC transitions.

	τ_{peak}	υ_{LSR} km s^{-1}	$\Delta\upsilon$ km s^{-1}	$\int\tau d\upsilon$ km s^{-1}	$N_{J_l} \times 10^{13}$ cm^{-2}
CCC					
$Q(2)$	0.53	63.9(1)	11.6(2)	6.6(1)	32.6(5)
$Q(4)$	0.56	64.4(1)	13.7(2)	8.3(1)	40.9(5)
$Q(6)$	0.87	64.3(1)	12.5(1)	11.5(1)	56.6(5)
$P(2)$	0.15	63.5(3)	12.7(8)	2.0(1)	49.8(25)
$P(4)$	0.34	63.8(1)	12.5(3)	4.5(1)	67.8(15)
$P(6)$	0.39	63.4(1)	12.5(3)	5.2(1)	68.5(13)
$P(8)$	0.31	64.4(1)	13.0(4)	4.2(1)	52.1(12)
$P(10)$	0.24	65.7(2)	11.7(4)	2.9(1)	34.9(12)
$P(12)$	0.15	65.5(4)	13.0(8)	2.1(1)	24.8(12)
C^{13}CC $^{(a)}$					
$Q(2)$	0.046	62.0(3)	10.8(7)	0.53(3)	2.64(15)
$Q(4)$	0.040	62.0(4)	10.8(10)	0.46(4)	2.28(20)
^{13}CCC					
$Q(2)$	0.027	62.8(8)	11.1(15)	0.32(4)	1.58(20)
$Q(4)$	0.021	62.9(3)	11.6(6)	0.26(1)	1.26(5)

Notes. $^{(a)}$Only H-polarization data was used.

Rotational Diagram of C_3 CCC, ^{13}CCC and C^{13}CC

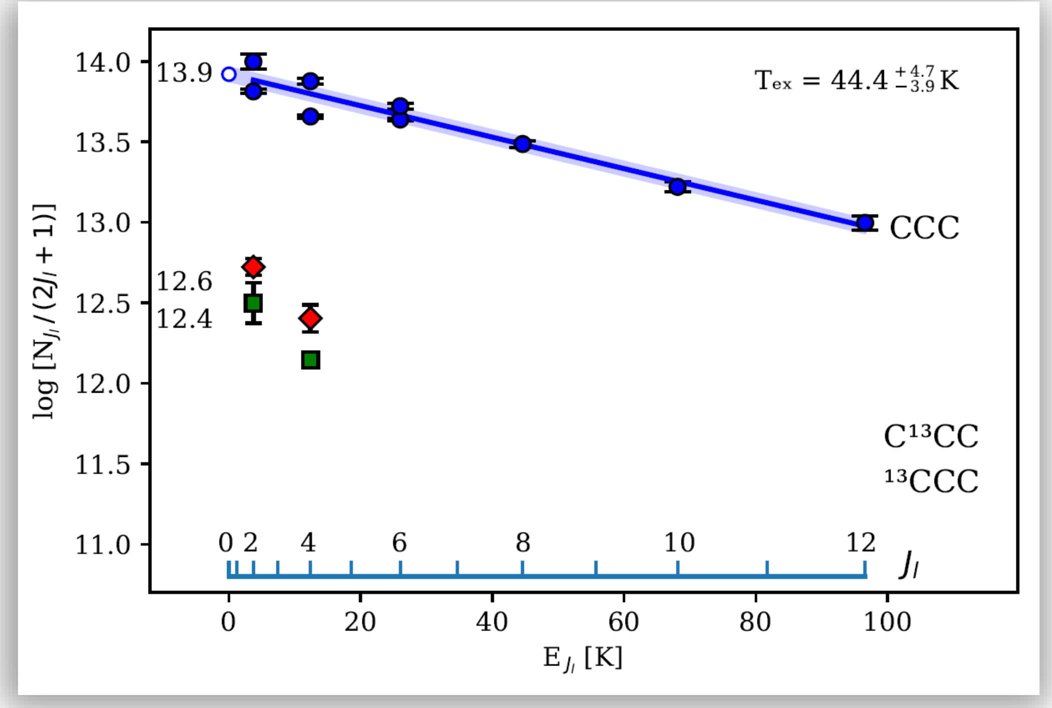

$$N_{J_l} = \frac{8\pi\nu^3}{c^3}\frac{g_l}{A_{ul}\,g_u}\left[1-\exp\left(-\frac{h\nu}{k_B T_{ex}}\right)\right]^{-1}\int\tau d\upsilon$$

Eq (1)

T. F. Giesen, B. Mookerjea, G. W. Fuchs, A. A. Breier, D. Witsch, R. Simon, J. Stutzki, A&A 2020, **633,** A120

Data Analysis of C_3 CCC, ^{13}CCC and C^{13}CC

Table 3. Summary of observed and derived quantities for the CCC, C^{13}CC, and ^{13}CCC transitions.

	τ_{peak}	υ_{LSR} km s^{-1}	$\Delta\upsilon$ km s^{-1}	$\int \tau d\upsilon$ km s^{-1}	$N_{J_l} \times 10^{13}$ cm^{-2}
CCC					
$Q(2)$	0.53	63.9(1)	11.6(2)	6.6(1)	32.6(5)
$Q(4)$	0.56	64.4(1)	13.7(2)	8.3(1)	40.9(5)
$Q(6)$	0.87	64.3(1)	12.5(1)	11.5(1)	56.6(5)
$P(2)$	0.15	63.5(3)	12.7(8)	2.0(1)	49.8(25)
$P(4)$	0.34	63.8(1)	12.5(3)	4.5(1)	67.8(15)
$P(6)$	0.39	63.4(1)	12.5(3)	5.2(1)	68.5(13)
$P(8)$	0.31	64.4(1)	13.0(4)	4.2(1)	52.1(12)
$P(10)$	0.24	65.7(2)	11.7(4)	2.9(1)	34.9(12)
$P(12)$	0.15	65.5(4)	13.0(8)	2.1(1)	24.8(12)
C^{13}CC [a]					
$Q(2)$	0.046	62.0(3)	10.8(7)	0.53(3)	2.64(15)
$Q(4)$	0.040	62.0(4)	10.8(10)	0.46(4)	2.28(20)
^{13}CCC					
$Q(2)$	0.027	62.8(8)	11.1(15)	0.32(4)	1.58(20)
$Q(4)$	0.021	62.9(3)	11.6(6)	0.26(1)	1.26(5)

Notes. [a] Only H-polarization data was used.

$$N_{J_l} = \frac{8\pi\nu^3}{c^3}\frac{g_l}{A_{ul}\,g_u}\left[1-\exp\left(-\frac{h\nu}{k_B T_{ex}}\right)\right]^{-1}\int \tau d\upsilon$$

Eq (1)

Rotational Diagram of C_3 CCC, ^{13}CCC and C^{13}CC

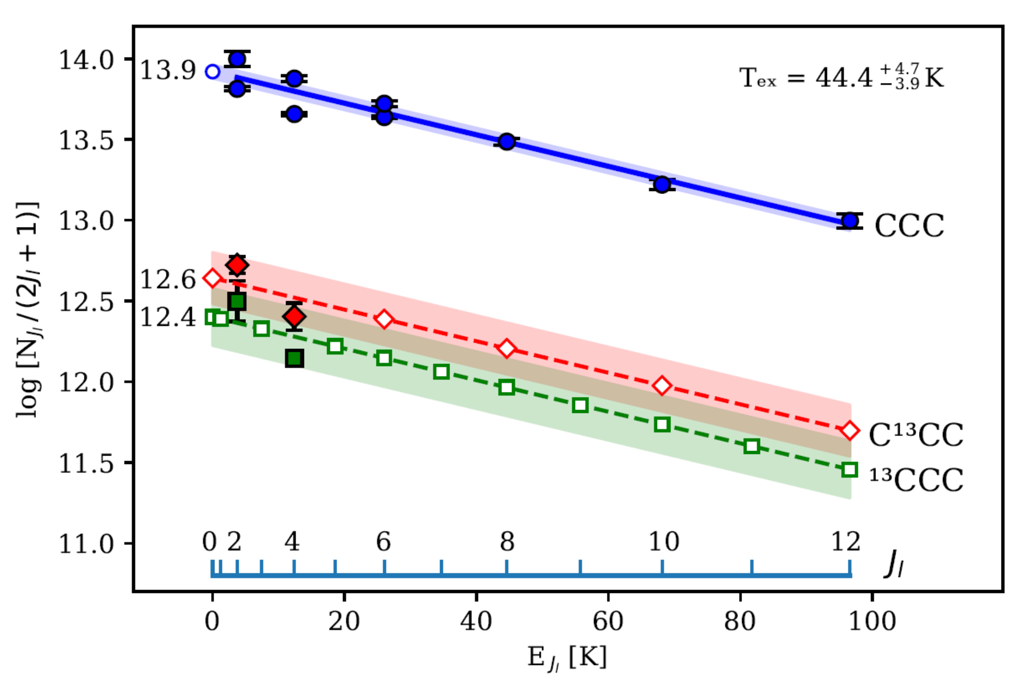

	T_{ex}(K)	log (N_0)	Q_{rv}	$N \times 10^{14}$ cm^{-2}	rel.
CCC	$44.4^{+4.7}_{-3.9}$	13.92(04)	46.64	$38.8^{+3.9}_{-3.5}$	100%
C^{13}CC	44.4	12.64(16)	47.66	$2.1^{+0.9}_{-0.6}$	5 ± 2%
^{13}CCC	44.4	12.40(18)	97.30	$2.4^{+1.2}_{-0.8}$	6 ± 3%

$$Q_{rv} = \sum_{J_l(v=0,1,2)} (2J_l+1)\,g_v \exp\left(\frac{-E_{rv}(J_l, v)}{k_B T_{ex}}\right)$$

Eq (2)

T. F. Giesen, B. Mookerjea, G. W. Fuchs, A. A. Breier, D. Witsch, R. Simon, J. Stutzki, A&A 2020, **633**, A120

Results for $^{12}C/^{13}C$ Ratios

	T_{ex}(K)	log (N_0)	Q_{rv}	$N \times 10^{14}$ cm^{-2}	rel.
CCC	$44.4^{+4.7}_{-3.9}$	13.92(04)	46.64	$38.8^{+3.9}_{-3.5}$	100%
$C^{13}CC$	44.4	12.64(16)	47.66	$2.1^{+0.9}_{-0.6}$	5 ± 2%
^{13}CCC	44.4	12.40(18)	97.30	$2.4^{+1.2}_{-0.8}$	6 ± 3%

$$N = Q_{rv} \frac{N_{J_1}}{2J_1 + 1} \exp\left(\frac{E_{rot}(J_1)}{k_B T_{ex}}\right)$$

Eq (3)

MEASURED RATIO

$N(CCC) : N(^{13}CCC) : N(C^{13}CC)$

18.6 : 1.2 : 1.0

EXPECTED RATIO

$N(CCC) : N(^{13}CCC) : N(C^{13}CC)$

20 : 2.0 : 1.0

MEASURED RATIO

$$\frac{^{12}C}{^{13}C} = \frac{3N(CCC)}{N(^{13}CCC)+N(C^{13}CC)} = 25.8$$

EXPECTED RATIO

$$\frac{^{12}C}{^{13}C} = 20$$

Total vs. Line by Line Ratio of Column Densities

N^a/N^b	$\frac{N(CCC)}{N(C^{13}CC)}$	$\frac{N(CCC)}{N(^{13}CCC)}$	$\frac{N(^{13}CCC)}{N(C^{13}CC)}$	$\frac{^{12}C}{^{13}C}$
TOTAL	18.6(7.0)	16.0(6.7)	1.2(0.6)	25.8(7.5)
$Q(2)$	12.1(0.7)	9.9(1.3)	1.2(0.2)	16.3(1.2)
$Q(4)$	17.6(1.6)	15.6(0.6)	1.1(0.1)	24.7(1.2)
AV	14.8(2.7) [a]	12.7(2.8) [a]	1.2(0.1) [a]	20.5(4.2) [a]
EXPEC	20	10	2	20

Line by Line Ratio of Column Density

$$\frac{N(a)}{N(b)} = \frac{Q^a_{rv}\, N^a_{J_1}\, (2J^b_1 + 1)}{Q^b_{rv}\, N^b_{J_1}\, (2J^a_1 + 1)} \cdot \exp\left(\frac{\Delta E_{rot}}{k_B T_{ex}}\right)$$

Eq (4)

T. F. Giesen, B. Mookerjea, G. W. Fuchs, A. A. Breier, D. Witsch, R. Simon, J. Stutzki, A&A 2020, **633,** A120

Exchange and Rearrangement Reactions

$$X(^{12}C) + {}^{13}CCC \rightleftharpoons C^{13}CC + X(^{12}C) + \Delta E_0 \quad \text{Eq (5)}$$

Equilibrium Reaction Rate

$$k_p = \exp\left(\frac{-\Delta G}{k_B T_{ex}}\right) = \frac{Q^{\,^{13}CCC}}{Q^{\,C^{13}CC}} \exp\left(\frac{-\Delta E_0}{k_B T_{ex}}\right) \quad \text{Eq (6)}$$

ΔG = Difference in Gibbs energy
ΔE_0 = Difference in zero point energy

Low Temperature Equilibrium at 44 K

$$\frac{N(^{13}CCC)}{N(C^{13}CC)} = \frac{1.4}{1} \qquad \textit{measured}: \frac{1.2}{1}$$

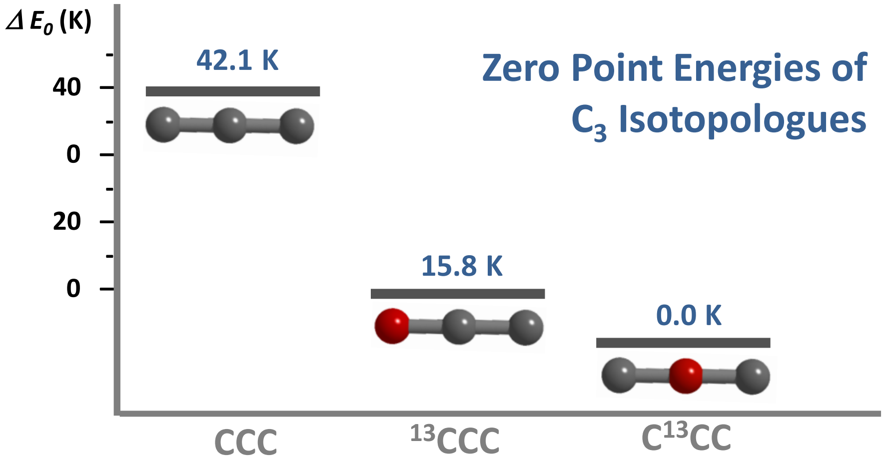

- **At low temperatures of 44 K the $N(^{13}CCC)/N(C^{13}CC)$ ratio shifts from 2.0 to 1.4, which is in much better agreement with the measured ratio of 1.2(1)**
- **The $^{12}C/^{13}C$ ratio in SgrB2(M) derived from C_3 isotopologues is 20.5 +/- 4.2, which is in good agreement with the result of 20 derived from earlier measurements**
- **Need of further $^{13}C_3$ measurements with SOFIA in other astronomical sources, including higher *J*-transitions**

T. F. Giesen, B. Mookerjea, G. W. Fuchs, A. A. Breier, D. Witsch, R. Simon, J. Stutzki, A&A 2020, **633,** A120